WPJET1-CPR(17) 17271

S Saarelma et al.

Integrated modelling of H-mode pedestal and confinement in JET-ILW

Preprint of Paper to be submitted for publication in Proceeding of 44th European Physical Society Conference on Plasma Physics (EPS)

This work has been carried out within the framework of the EUROfusion Consortium and has received funding from the Euratom research and training programme 2014-2018 under grant agreement No 633053. The views and opinions expressed herein do not necessarily reflect those of the European Commission.

Integrated modelling of H-mode pedestal and confinement in JET-ILW

S. Saarelma[1], C.D. Challis[1], L. Garzotti[1], L. Frassinetti[2], C.F. Maggi[1], M. Romanelli[1] C. Stokes[1,3] and JET Contributors*

EUROfusion Consortium, JET, Culham Science Centre, Abingdon, OX14 3DB, UK

1. CCFE, Culham Science Centre, Abingdon OX14 3DB, UK

2. Department of Fusion Plasma Physics, School of Electrical Engineering, KTH Royal Institute of Technology, SE-10044 Stockholm, Sweden

3. Department of Physics, University of Bath, Bath, BA2 7AY, UK

E-mail: samuli.saarelma@ukaea.uk

Abstract.

A pedestal prediction model Europed is built on the existing EPED1 model by coupling it with core transport simulation using Bohm-gyroBohm transport model to self-consistently predict JET-ILW power scan for hybrid plasmas that displays weaker power degradation than the IPB98(y,2) scaling. The weak power degradation is reproduced in the coupled core-pedestal simulation. The coupled core-pedestal model is further tested for a 3.0MA plasma with the highest stored energy achieved in JET-ILW so far, giving a prediction of the stored plasma energy within the error margins of the measured experimental value. A pedestal density prediction model based on the neutral penetration is tested on a JET-ILW database giving a prediction with an average error of 17% from the experimental data when a parameter taking into account the fuelling rate is added into the model. However the model fails to reproduce the power dependence of pedestal density implying missing transport physics in the model.

The future JET-ILW deuterium campaign with increased heating power is predicted to reach plasma energy of 11 MJ, which would correspond to 11-13 MW of fusion power in equivalent deuterium-tritium plasma but with isotope effects on pedestal stability and core transport ignored.

1. Introduction

The tokamak high confinement (H-mode) plasma inside the last closed flux surface can be divided in two distinct regions: The core that covers most of the plasma volume and is characterised by turbulent transport of heat and particles and relatively shallow gradients, and the pedestal that is a narrow region near the plasma edge where the ion scale turbulence is mostly suppressed leading to very a steep pressure gradient. The core density and temperature profiles are regulated mainly by transport processes, while in the pedestal MHD instabilities causing intermittent relaxations of the pressure gradient or edge localised modes (ELMs) play an important role limiting the pressure.

The resulting total pressure profile (and fusion power that depends roughly as $P_{fus} \propto p_0^2$) is a combination of these two regions. However, the regions cannot be predicted in isolation from each other. The reason for this is that the pedestal affects the core and the core affects the pedestal. Since

***See the author list of Litaudon et al, Overview of the JET results in support to ITER, accepted for publication in Nuclear Fusion**

the core temperature profile is usually set by turbulence whose drive is proportional to the normalised temperature gradient, $\nabla T/T$, and the height of the temperature pedestal sets the boundary condition, the achievable core temperature is strongly dependent on the pedestal value. On the other hand, the increasing the core pressure increases the Shafranov-shift, which in turn has a stabilising effect on the pedestal limiting peeling-ballooning modes (PBM) [1,2]. This feedback loop makes it essential to solve the pedestal and core self-consistently.

In this paper we show self-consistent core-pedestal simulations of a JET power scan and compare the results to the experiment. Furthermore, we give predictions for future JET experiments.

For the pedestal prediction we use the Europed model that is based on the idea of EPED [3] where the pedestal pressure is assumed to be limited by the combination of kinetic ballooning modes (KBM) and peeling-ballooning modes. In Europed we use the EPED1 scaling to connect the pedestal height and width: $\Delta = 0.076\sqrt{\beta_{p,ped}}$, where $\beta_{p,ped}$ is the poloidal β at the top of the pedestal and Δ is the pedestal width in normalised poloidal flux which is assumed to be the same for density and temperature profiles. Using this condition a range of pedestal with varying widths and corresponding heights are created and the peeling-ballooning stability of the equilibria is solved with an MHD stability code. The pedestal prediction is given at the pedestal where the criticality criterion for the fastest growing peeling-ballooning mode $\gamma = \gamma_{crit}$ is reached. In this work, we use a bilinear model for γ_{crit} similar to the EPED1.6 model [4]:

$$\gamma_{crit} = \begin{cases} \frac{\omega^*}{2}, n \leq 10 \\ \frac{\omega^*}{2}(n=10), n>10 \end{cases} \quad (1)$$

Where ω^* is the average diamagnetic frequency defined as half of the maximum diamagnetic frequency in the pedestal region.

The EPED model has two parameters that are not usually known in advance of the experiment, total plasma β and pedestal density. In section 2, we test two density pedestal models for predictive pedestal modelling. The first is based on the parameterisation of the large JET-ILW (ITER-like wall) database. The parameterisation uses only engineering parameters that are known before the experiment and can be useful for predicting pedestals in JET-ILW. Naturally it has limited usability in other devices as it contains no physical model. The second model is more physics based relying the density pedestal height to be set by the depth the neutrals penetrate into the pedestal from the scrape-off layer.

In section 3, we introduce a way to solve the core-pedestal problem self-consistently, thus avoiding having to know β in advance. Finally, we validate the new models using experimental JET plasmas and make predictions for future JET campaigns with more available heating power.

2. Pedestal density prediction

In EPED model, the pedestal density is given as input and only the temperature is predicted. This is a valid approach if the density can be controlled as a feedback parameter, ie. the target density is specified in advance of the experiment and the controls, eg. gas fuelling or pellets are adjusted to reach the target. This assumes that the density pedestal reacts to gas fuelling by increasing with increased fuelling; however, this is not always the case. For instance, in JET-ILW gas scans the

fuelling was varied from 0.2 to 3.8 × 10^{22} el/s with very little effect on the pedestal density height [5]. Furthermore, a minimal fuelling level may be required to protect the divertor and/or to keep ELM frequency high enough to avoid impurity accumulation. Therefore, we would like to predict the pedestal density along with the temperature.

The density in the pedestal is regulated by various processes such as neutral fuelling from outside the plasma, recycling from walls and divertor, pumping, particle transport between ELMs, particle losses during ELMs and particle flux from the core. Modelling all these processes self-consistently is a task beyond the scope of this paper. However, as a first step towards pedestal density modelling, we have used two simplified approaches to predict the density for given plasma parameters: pedestal density parameterisation and model based on neutral penetration.

The parameterised pedestal density is based on the analysis of JET-ILW database by Urano [6]. In this approach the pedestal density is given by a fitted formula containing only engineering parameters of the plasma:

$$n_{e,ped}[10^{19}m^{-3}] = 11.4 \cdot I_p^{1.38} \cdot B_t^{-0.42} \cdot P_{NBI}^{-0.25} \cdot \delta^{0.71} \cdot \Phi_e^{0.11} \quad (2)$$

where I_p is the plasma current [MA], B_t is the vacuum toroidal magnetic field [T], δ is the plasma triangularity P_{NBI} is the NBI heating power [MW] and ϕ_e is the fuelling rate [10^{22} s^{-1}]. As can be seen the coefficients for heating and fuelling are very small. So, the parameterisation is relatively insensitive to them, while the plasma current has the most significant effect on the pedestal density.

The parameterisation does not contain any physics insight and can only be used for the device the experimental data was collected from. Just changing the wall material from Beryllium/Tungsten to Carbon changes the parameterisation for JET. Therefore, it has little value on predicting density in devices that do not exist, such as ITER. As a more physics based approach we have used the neutral penetration model [7]. This model assumes that all the fuelling is from the plasma edge and that the particle diffusion coefficient D is constant in space and leads to a relation between the width Δ_{ne} in real units on the midplane and height $n_{e,ped}$ of the pedestal:

$$\Delta_{ne} = 2V_n / \left(\sigma_i V_e E n_{e,ped}\right), \quad (3)$$

where V_n is velocity of the neutral particles, σ_i is the cross section for electron impact ionization and V_e is the electron thermal velocity. The factor E represents the flux expansion between the fuelling location (usually near the X-point) and the midplane where the pedestal width is evaluated. Eq. 3 gives the width in real space, which is then mapped to flux space using the equilibrium information. V_n is calculated taking into account Frank-Condon and charge-exchange neutrals using the formulas [8]:

$$v_{CE} = \sqrt{\frac{T_i}{2\pi m_i}} \quad (4)$$

$$v_{FC} = \frac{2}{\pi}\sqrt{\frac{3}{m_i}} \quad (5)$$

$$w = \frac{\frac{v_{FC}}{2}\sigma_i V_e}{\left(v_{FC}\sigma_i V_e - v_{CE}\sigma_i V_e - v_{CE}\sigma_{CE} V_e\right)} \quad (6)$$

$$v^{i} = \frac{\left(v_{FC}\sigma_i V_e + \frac{v_{CE}\sigma_{CE} V_e}{2} \right)}{\left(\sigma_i V_e + \frac{\sigma_{CE} V_e}{2} \right)} \quad (7)$$

$$V_n = \frac{v_{FC} w + v^{i}}{w+1} \quad ,(8)$$

where $\sigma_i V_e$ is the ionization rate coefficient, $\sigma_{CE} V_e$ the charge exchange rate coefficient, V_{FC} the velocity of the Frank–Condon neutrals, V_{CE} the velocity of the charge exchange neutrals and w is the ratio of charge exchange to Frank–Condon neutrals reaching the separatrix. The ionisation and charge exchange rate coefficients are calculated using the pedestal temperature and the rates as a function of particle energy in [9].

As in EPED1 in Europed we assume that $\Delta_{ne}=\Delta_{Te}=\Delta$. So for a given pedestal width and temperature, the density pedestal height can be solved from Eqs. 3-8.The full calculation is done in an iterative loop as the total pedestal pressure for a given pedestal width is constrained by the $\Delta = 0.076\sqrt{\beta_{p,ped}}$ condition requiring to adjust the pedestal temperature as a response to a newly calculated pedestal density to keep $\beta_{p,ped}$ fixed.

Before implementing the full iteration into Europed, we tested just the feasibility of the neutral penetration scheme for the JET pedestal database. We selected 208 JET-ILW well-diagnosed discharges with I_p=2-2.5 MA, B_t=2.2-2.65T, δ=0.25-0.4, and calculated the density pedestal value using the measured pedestal width and the temperature pedestal along with the global parameters. The pedestal profiles were measured using the Thomson scattering diagnostic and the parameters (width and height) obtained from a fit to a modified hyperbolic tangent function using the methods described in [10] As shown in Fig. 1.when we used a fixed value E=5 (based on MAST results in [8]) for the flux expansion factor, the model gives a match to the average of the data, but does not reproduce the variation. It under-predicts the pedestal at high density and over-predicts at low density. Note that the fuelling rate does not enter this calculation at all and the heating power enters in only through the pedestal temperature.

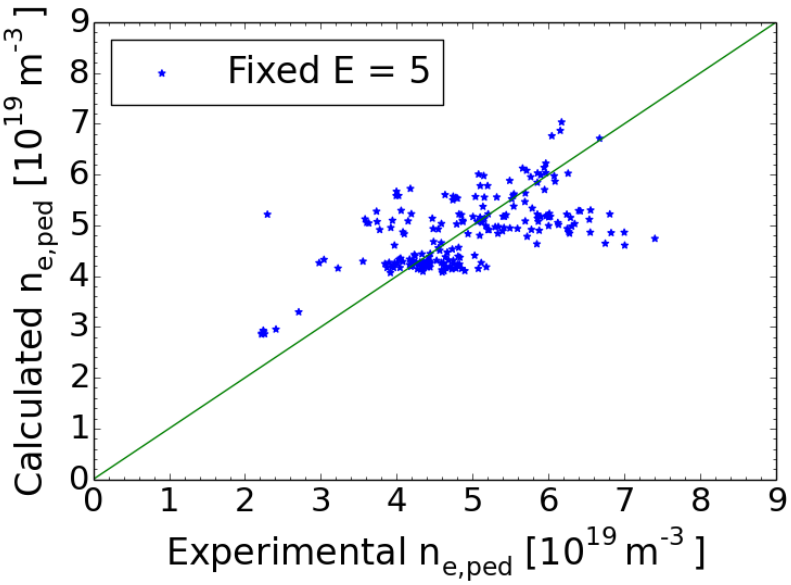

Figure 1. The pedestal density calculated using the neutral penetration model and a fixed value of E=5 as a function of experimental pedestal density for 208 JET-ILW H-mode plasmas. The line indicates equal calculated value to the experimental value.

To improve the model at high density, we introduce fuelling dependence on the flux expansion factor E:

$$E = A\,\Phi^{-b}, \quad (9)$$

Where Φ is the total gas fuelling rate in 10^{22} el/s. The parameters are fitted to the data and are A=5.3±0.3 and b=-0.17±0.05. While the parameters here are chosen to improve the fit on the data, there is a physical justification for the flux expansion parameter to vary with fuelling rate. At low gas rate most of the neutrals enter the plasma through the X-point, which means that *E* is at its maximum. As the fuelling is increased, neutrals start entering the plasma further and further from the X-point lowering *E*. Using this method of taking into account the effect of the fuelling rate on the density, we recalculate the pedestal density. This is shown in figure 2 together with the density calculated from the parameterisation (Eq. 2). The average error for the calculated parameterised density and neutral penetration model is 12% and 11%, respectively.

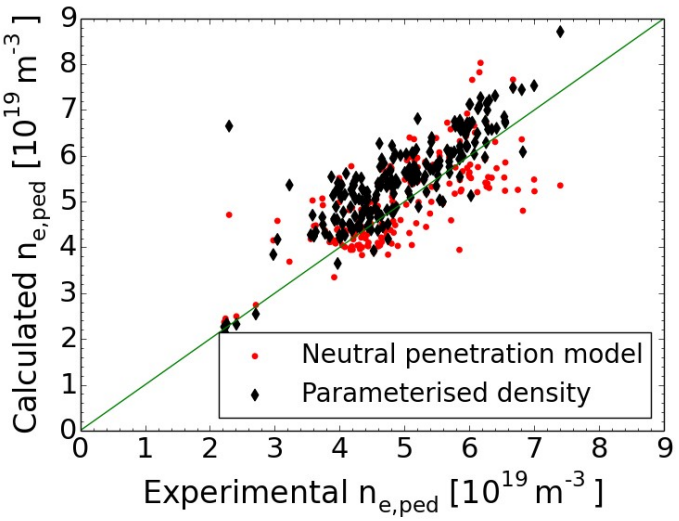

Figure 2.The pedestal density calculated using the neutral penetration model and a flux expansion factor varying with fuelling rate (Eq.4, red circles) and the parameterised density (Eq. 2, black diamonds) as a function of experimental pedestal density.

So, if the temperature pedestal height and the pedestal width are known, the neutral penetration model with the inclusion of the gas rate dependence, can predict the JET-ILW H-mode density relatively well. However, in true prediction we do not know them in advance. We have run 28 cases from the above database using Europed with both density pedestal models combined with the standard EPED1 prediction of the temperature. As shown in Fig. 3., both models predict the density reasonably well. The average error is 17% for neutral penetration model and 17% for the parameterised density.

In addition to pedestal density, the separatrix density $n_{e,sep}$ is a free parameter in the EPED1 model. However, it has very little effect on the predicted pedestals. A scan of $n_{e,sep}$=0.1-0.5×$n_{e,ped}$ gave a variation of less than 0.5% in the predicted pedestal top pressure.

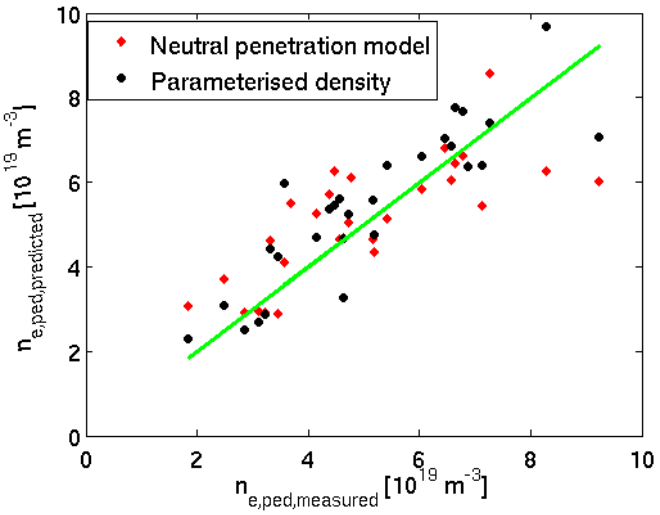

Figure 3. Predicted density in a full Europed run for 28 JET-ILW H-mode plasmas using the two model: parameterised density (black diamonds) and neutral penetration model (red circles). The diagonal line indicates where the prediction is equal to the experiment.

3. Self-consistent core-pedestal transport model

In the EPED model, the global β is assumed to be known in advance. While this may be a reasonable approach in experiments that are done in a so-called β feedback mode, ie. the power is adjusted to match the target β, often in experiments the total heating power waveform is set in advance and resulting β is a result of the experiment. Furthermore, when trying to reach the limits of the performance, the experiments are run at maximum power giving no flexibility in adjusting the power. In the cases where the heating power instead of β is known, the core temperature profiles T_i, T_e, have to be predicted using a steady-state transport model for electrons (e) and ions (i) [11]:

$$\frac{\partial T_{e,i}}{\partial \varrho} = \frac{-q_{e,i}}{V' \left\langle |\nabla \varrho|^2 \right\rangle n_{e,i} \chi_{e,i}} \quad (10)$$

where χ is the diffusivity, V'=dV/dρ is the radial derivative of the plasma volume, n is the density, q_e is the heat flux and ρ is a radial coordinate. In this work we use the Bohm-gyroBohm transport model [12] to obtain the diffusivities for given profiles and equilibrium since the JET-ILW core has indeed been found to follow the gyroBohm scaling [13]. It must be noted that the Bohm-gyroBohm model uses parameters fitted to JET L-mode data before the ITER-like wall was installed and not based on the first principle turbulence simulations.

The heat flux $q_{e,i}$ through each flux surface can be calculated from the source distribution:

$$q_{e,i}(\varrho) = \int_0^{V(\varrho)} P_{e,i} dV \quad (11)$$

where $P_{e,i}(\rho)$ is the absorbed power density profile.

In principle the core density profile could be predicted the same way using particle diffusion. However, the particle sources are harder to calculate than the heating sources. Furthermore, since we are not interested in fine details of the profile, but only need a rough estimate for the density profile peaking (n_0/n_{ped}), we take advantage of the parameterisation of the density peaking for given collisionality in [14] and solve the core density profile using the core temperature and pedestal density profiles:

$$n_{pk} = n(\square^{0.5} = 0.2) / \langle n \rangle = 1.347 - 0.117 * \ln(\square_{eff}) - 4.03 * ¿, \quad (12)$$

where ν_{eff} is the effective collisionality and is defined as $\nu_{eff} = 0.2 \langle n_{ped} \rangle R_0 / \langle T_e \rangle^2$ and $¿ 4.02 \times 10^{-3} \langle p \rangle / B_{T0}^2$, with $\langle p \rangle = 2 \langle T \rangle n_{ped}$ (in units of keV × 10^{19}m^{-3}).

The increasing density peaking with decreasing collisionality has been observed in JET-ILW plasmas [15, 16]. The simple model is likely to under-predict strongly NBI heated pulses as there the beam fuelling plays a role in density peaking [17], but we still note here that even if the calculation of the core density peaking has an error, this is compensated by the temperature profile (Eq. 10). If the density profile peaking is over-predicted, the core temperature will be less peaked and vice versa and as a result the total β will not be strongly affected. As the pedestal stability is affected by core pressure and not the temperature or density profiles, the effect will be small on pedestal prediction. Furthermore, unlike in a complete transport simulation, this approach does not require knowing the density sources and sinks, which are generally not as easy to calculate as the heating sources.

In Europed this method is implemented by specifying the heating source amplitude and profile and solving the temperature profile using Eq. 10 and 11 with the given pedestal temperature as the boundary condition. This is then used to calculate the core density profile from Eq 12. The process is repeated until it converges. A new equilibrium is calculated with the new profiles assuming that the current is a combination of fully diffused inductively driven current calculated from the neo-classical conductivity profile and the bootstrap current calculated using formulas in [18,19] and this is continued until the profiles and the equilibrium are self-consistent. This is done for a range of hypothetical pedestals (consistent Δ and $\beta_{p,ped}$). The stability of the equilibria is solved and the final prediction is obtained at the point of criticality ($\gamma = \gamma_{crit}$).

The used bootstrap current model has some effect on the pedestal prediction. The error margins given in the Europed predictions in Sec 4. correspond to the variation in predictions due to bootstrap current model.

Since all the calculations are done inside Europed iteration, this is relatively fast method resulting a prediction within 1 hour of wall time with parallelisation used to solve each hypothetical pedestal width separately. While it can give a rough estimate of the pedestal and total β, a more sophisticated result is obtained by combining the pedestal prediction with a proper transport code that solves the heating profiles, energy exchange between particle species. In this work, we have used JINTRAC [20] code along with Europed. The radiated power from the plasma is not modelled but taken from the bolometry measurements of the experiment. In the extrapolations to high power, we have assumed that the radiated power stays constant as the heating power is increased, which is consistent with the power scan experiment, where very weak (0.6MW increase in radiated power for an increase of 8MW of heating power) was observed.

The self-consistent core-pedestal integration can be done in two ways. The straightforward way is to pass information between the codes (global β to the pedestal prediction, pedestal height to the core prediction) and iterate until converged. This is similar to the method used by Meneghini et al. for DIII-D and ITER prediction in [21], where TGLF core transport model was used together with EPED1 pedestal prediction. It is a relatively slow method as a new core iteration cannot be run at a same time with a new pedestal iteration. However, since we know that the main effect for the core to affect the pedestal is the β-stabilisation and the main effect for the pedestal to affect the core is by giving the core transport simulation a boundary condition, the iteration can be replaced by two scan: The core simulation is repeated with a range of pedestals and the pedestal simulation is repeated with a range of global β values. The self-consistent solution for the coupled pedestal-core prediction is found at the pedestal height and global b values that are consistent for both scans are shown schematically in Fig. 4. As long as the solution is unique, both methods converge to the same solution.

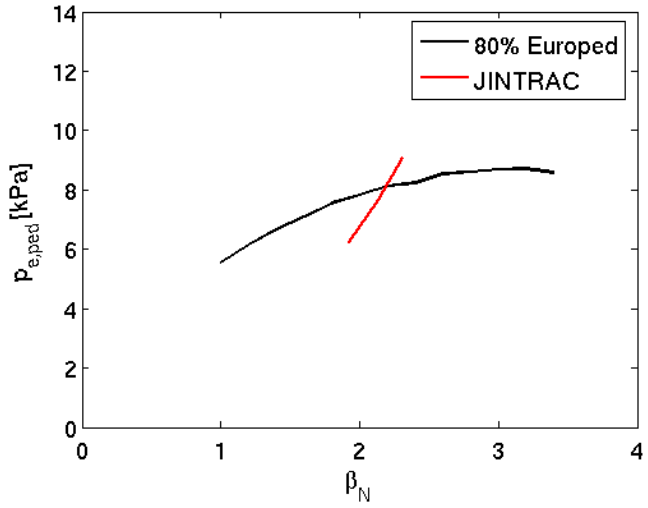

Figure 4. A schematic picture showing a way to find a self-consistent solution to the coupled core-pedestal prediction problem. Pedestal pressure is predicted for a range of global β values with Europed (black line). Global β is predicted for a range of pedestal pressures as a boundary condition using JINTRAC (red line).The crossing points of the red and the black lines correspond to the self-consistent solution.

The pedestal prediction based on the marginal peeling-ballooning stability gives the pedestal just before an ELM crash. However, the effect of ELMs is not taken into account in the steady-state transport simulation. In the coupled simulation we correct this by assuming that the ELM averaged pedestal density and temperature heights are 10% lower than the pre-ELM pedestal values, which

4. Predictions for JET-ILW plasmas

We use the coupled core-pedestal prediction on the JET-ILW power scan (P=4.6-12.4MW) at I_p=1.4 MA, B_t=1.7 T, low triangularity (δ≈0.25) and low gas fuelling reported in [22, 23]. This dataset was chosen because in the previous study [2, 23] we had found that the experimental plasmas were close to the peeling-ballooning stability boundary before an ELM crash. Datasets that are below the stability limits (eg. similar power scan at high gas rate [22]) are unlikely to be reproduced by a predictive model that assumes that the solution is found at marginal peeling-ballooning stability. Since we're interested in how well the coupled core-pedestal model works, we do not predict the density as was described in Sec. 2 but use the experimental pedestal density instead.

We first do the pedestal prediction part. Figure 5 shows the predicted pedestal pressure as a function of global β_N. The scan is repeated for a range of pedestal densities that correspond to different experimental pedestals, but as can be seen, it has little effect on the predicted pedestal pressure. Regardless of the density the pedestal predictions match very well the trend of the experiment. The increase in predicted pedestal height with β_n is due to improved pedestal stability with increasing Shafranov-shift as is shown in Fig 6 where the stability boundaries for two Europed predicted pedestals at different β_n are depicted.

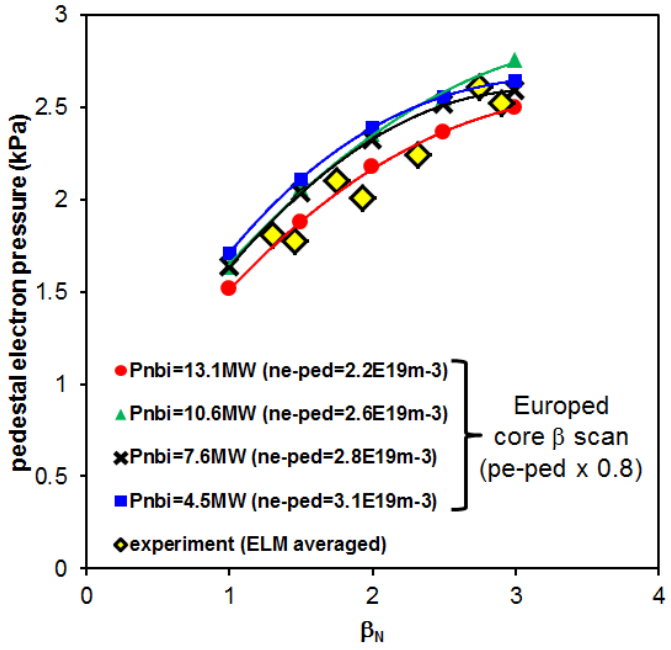

Figure 5. Predicted pedestal electron pressure as a function of global β_N for various experimental densities (lines) and the experimental pedestal electron pressure (yellow diamonds).

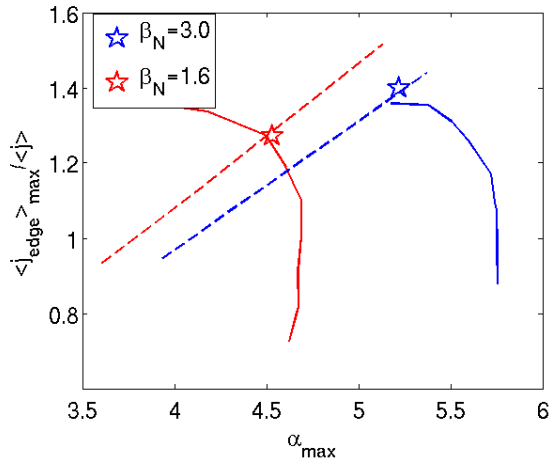

Figure 6. The peeling –ballooning stability boundaries (solid lines) for predicted pedestals at β_N=3.0 (blue) and β_N=1.6 (red) in normalised pressure gradient (α) and edge current density (j) space. The dashed lines show the path that the equilibria with $\Delta = 0.076\sqrt{\beta_{p,ped}}$ follow for both cases and the stars represent the marginally stable equilibrium.

Next we combine the pedestal prediction with the core simulation to produce the full self-consistent pedestal-core solution. In Fig. 7., the coupled core-pedestal simulation thermal stored energy and energy confinement time are compared with the experiment. The experimental stored thermal energy values are an average of three types of measurements, (1) W_{dia}-1.5$W_{fast,\perp}$, (2) W_{MHD}-0.75$W_{fast,\perp}$-1.5$W_{fast,\parallel}$ and (3) integral of kinetic profiles, where W_{dia} is the measured diamagnetic energy, W_{MHD} is the plasma energy from the equilibrium reconstruction and W_{fast} is the total fast particle energy in an interpretative TRANSP [24] simulation. The error bars represent the variation between the three methods. While the core-pedestal simulation slightly over-predicts the total thermal energy in the plasma and the thermal confinement time, the dependency with the power is very well matched with

the experiment. Furthermore, the predicted and the experimental trends differ from the IPB98(y,2) H-mode scaling law [25] that has stronger power degradation than the experiment and the simulation and confirms the physical mechanism of pedestal-core synergy described in [23].

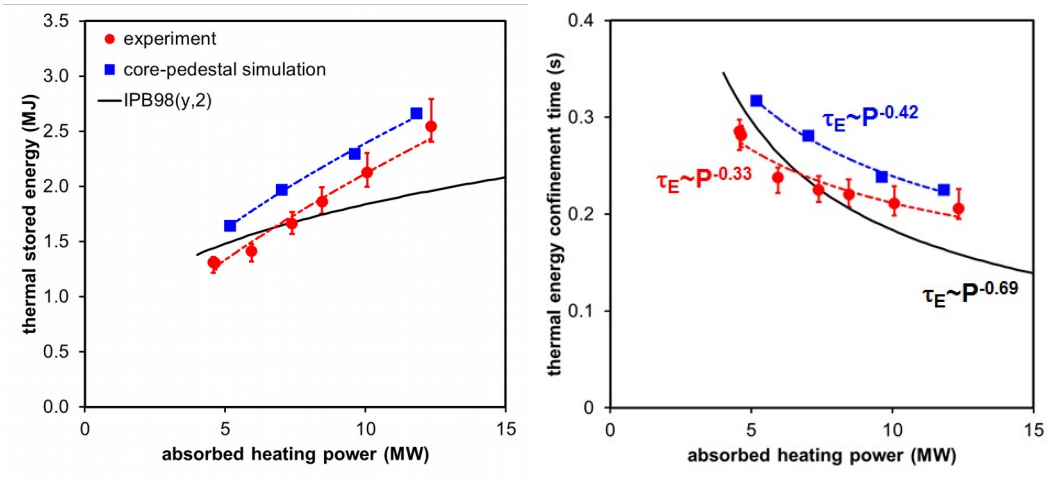

Figure 7. The predicted (blue squares) and experimental (red circles) thermal energy (left) and energy confimement time (right) as a function of absorbed heating power. For comparison the IPB98(y,2) power dependency is shown (black line).

When we combine the pedestal density prediction to the core-pedestal prediction, we find that the neutral penetration model does not reproduce the decreasing trend of density with power that is observed in the experiment and is in the parameterised density model as well. As shown in Fig. 8., the neutral penetration model predicts the average density in the power scan, but does not reproduce the trend with the power. This indicates that while the neutral penetration model works reasonably well for a large database, it is clearly missing some physics most likely associated with the particle transport in the pedestal and ELMs that can change significantly in such a power scan.

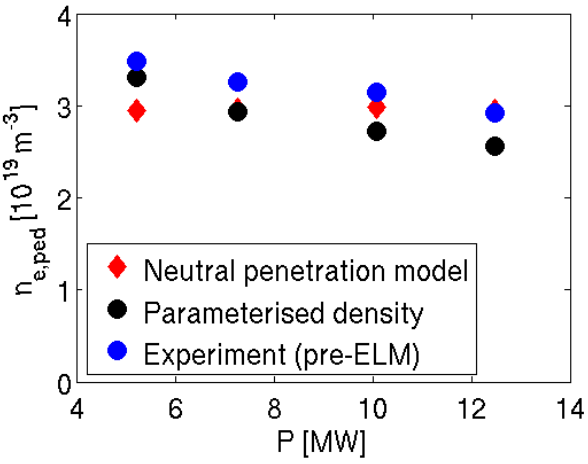

Figure 8. Predicted and measured pedestal density in the JET-ILW power scan.

Using the coupled core-pedestal simulation method, we expand our prediction to a JET-ILW discharge #86614, which has the same plasma shape that was used in the power scan, but has I_p=2.5MA, B_t=2.9T, β_N=2.3 and P=26MW. Furthermore, we extrapolate from this to a full power (P=38MW) that is expected to be available in the future JET campaigns. In Fig. 9 we can see that the

high current case is well reproduced by the coupled core-pedestal simulation. The full power (38MW) prediction for the total thermal stored energy in the plasma is 8.6± 0.4MJ and β_N=3.0± 0.1. Interpretive simulations of the fusion power based on the predicted plasma profiles and 50-50 deuterium-tritium (DT) plasma were performed using the JETFUSE code, which approximates the trajectory of the NBI system as a single, zero-width pencil in the plasma equatorial plane for beam deposition, and determines the fast ion slowing-down neglecting pitch-angle, orbit and rotation effects. The beam-target and thermal fusion reactions are modelled following [26, 27]. The predicted fusion power for the full power DT-equivalent case ignoring other isotope effects than the fusion cross-section is 13MW.

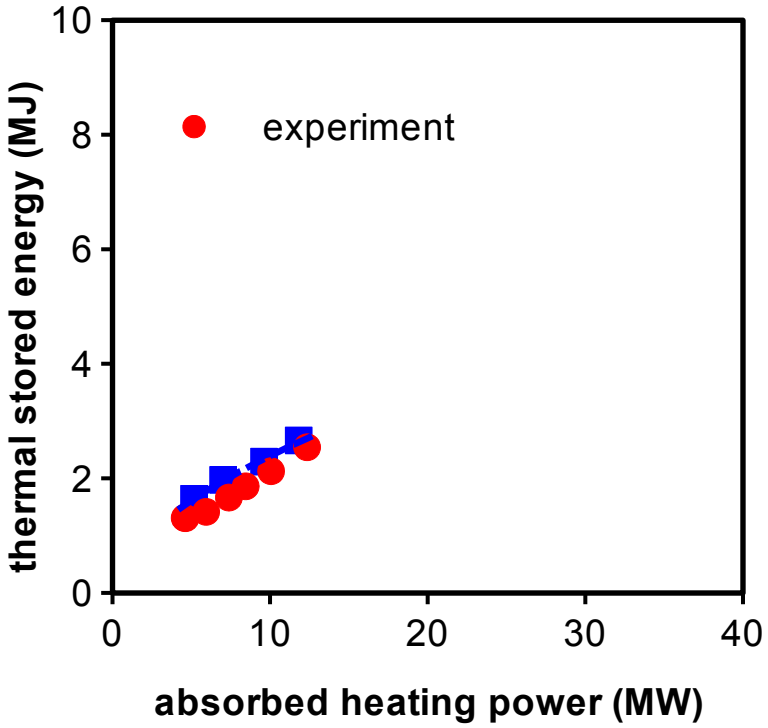

Figure 9. The predicted (blue) and measured (red) total thermal stored energy in JET-ILW plasmas. The highest power (38MW) point is a prediction for a future JET experiment. The error bars in the simulation result represent the uncertainty due to the bootstrap current model used and in the experimental results it is the variation between different methods of calculating the thermal stored energy.

The neutral penetration model in Europed gives the pedestal density prediction of $n_{e,ped}=5.5\times10^{19}m^{-3}$, which is higher than the measured $4.6\pm0.5\times10^{19}m^{-3}$ indicating that at high power neutral penetration model does not properly take into account the increased particle transport. The parameterised density model predicts the density within the error margins giving a value of $4.2\times10^{19}m^{-3}$.

Finally, we use the coupled core-pedestal method to simulate the discharge with the highest plasma stored energy achieved in JET-ILW so far, #92436. The global parameters for this discharge are I_p=3.0MA, B_t=2.8T, $\delta\approx0.20$, P=34MW, β_N=2.2 and $H_{98(y,2)}$=1.1. The main difference to the discharges simulated above (the power scan and #86614) is the lower edge safety factor, q_{95}, which is 3.6 for #86614 and 3.0 for #92436. The discharge is pellet fuelled and the ELMs in this discharge are not typical Type I ELMs. Since the ELMs in this discharge are very irregular, we are not able to compare

the pre-ELM pedestal profiles, but only the ELM averaged quantities. It must be noted, however, that similar pulses with gas fuelling have Type I ELMs and their ELM averaged pedestal parameters are very similar to the studied discharge. The total plasma energy in the experiment is 9.8 ±0.5 MJ and in the coupled pedestal-core simulation it is 9.7±0.6 MJ. Based on the good match with the experiment, we make an extrapolation for JET plasma at higher plasma current (3.4 and 3.8 MA), the toroidal magnetic field (3.1 and 3.46T) and increased heating power expected to be available in future JET campaigns (40MW). The density is scaled with the current in the prediction. The extrapolation results are collected into table 1. Using the profiles of the self-consistent prediction, we calculate the expected fusion power in equivalent DT-plasma. This calculation gives P_{fus}=11 MW for the highest current value. It must be noted, however, that no isotope effect on the pedestal stability or core transport is taken into account in this calculation. The recent JET experiments with hydrogen indicate increase in pedestal pressure height with increasing isotope mass [28]. These effects will be included into the core-pedestal prediction of a true DT-plasma in future work.

	Coupled core-pedestal simulation				Density pedestal prediction	
I_p [MA]	$W_{thermal}$ [MJ]	DT-equivalent P_{fus} [MW]	β_N	$p_{e,ped}$ (ELM-averaged) [kPa]	$n_{e,ped}$ (Neutral penetration model) [10^{19} m^{-3}]	$n_{e,ped}$ (parameterised density) [10^{19} m^{-3}]
3.0	8.4	7.5	2.3	8.3	6.1	5.8
3.4	9.6	9.5	2.0	10.9	7.2	6.3
3.8	11.0	11.2	1.8	12.8	8.0	7.0

Table 1. Predicted values of $W_{thermal}$,P_{fus}, β_N, $p_{e,ped}$,in a coupled core-pedestal simulation for the JET discharge #92436 (I_p=3.0MA,P_{AUX}=34MW) and the two extrapolated currents (I_p=3.4 and 3.8 MA) at P_{AUX}=40MW and $n_{e,ped}$ values in the density pedestal prediction with the two models.

We test the neutral penetration model in Europed on this discharge as well giving a value of $n_{e,ped}$=6.1 × 10^{19} m^{-3} while the ELM averaged experimental pedestal density is 5.2 ±0.5 × 10^{19} m^{-3}. The extrapolation to higher current, field and power while keeping the fuelling rate fixed gives a dependency of $n_{e,ped} \propto I_p^{1.15}$, which is close to the linear dependency with current used in the coupled pedestal-core extrapolation.

4. Conclusions

The coupled core-pedestal predictions using Europed for the pedestal and JINTRAC with Bohm-gyroBohm transport model for the core are able to reproduce the JET-ILW power scan at 1.4MA giving power degradation of confinement time very close to the experiment and lower than the IPB98(y,2) scaling. The experimental discharges at high current and power operation are also reproduced using the self-consistent core-pedestal modelling.

The pedestal density prediction based on the neutral penetration model augmented with a parameter taking into account the reduction in flux expansion factor as the gas fuelling is increased implemented in the Europed code is able to reproduce JET-ILW discharges with the error similar to the parameterisation of the pedestal density. However, the neutral penetration model fails to reproduce the decrease in pedestal density with power in a dedicated power scan indicating incomplete physics in

the model. Further work taking into account the particle transport in the pedestal is required to capture the power dependence in the pedestal density model.

Neglecting any effects from isotopes the projection using the self-consistent core-pedestal model for the fusion power for a deuterium-tritium JET plasma with I_p=3.8MA, B_t=3.46T and P=40MW is found to be 11MW and 13MW for the I_p=2.5MA, B_t=2.9T and P=38MW. Further modelling work for the isotope effects both in the core and pedestal is required to get a more accurate prediction for the highest actual fusion power achievable in JET.

Acknowledgements

This work has been carried out within the framework of the EUROfusion Consortium and has received funding from the Euratom research and training programme 2014-2018 under grant agreement No 633053 and from the RCUK Energy Programme [grant number EP/P012450/1]. The views and opinions expressed herein do not necessarily reflect those of the European Commission.

References:

[1] P.B. Snyder et al.,Nucl. Fusion **47** (2007) 961
[2] S. Saarelma et al., Phys. Plasmas **22** (2015) 056115
[3] P.B. Snyder et al. Phys. Plasmas **16** (2009) 056118
[4] P.B. Snyder et al., Nucl. Fusion **51** (2011) 103016
[5] M.J. Leyland et al., Nucl. Fusion **55** (2015) 013019
[6] H. Urano et al., Proc. 43rd EPS Conference on Plasma Physics, 4 - 8 July, 2016, Leuven, Belgium, O4.121
[7] R.J. Groebner et al., Phys. Plasmas **9** (2002) 2134
[8] A. Kirk et al., Plasma Phys. Control. Fusion **46** (2004) A187
[9] R.L. Freeman and E.M. Jones. Atomic collision processes in plasma physics experiments. (CLM-R 137), May 1974
[10] L Frassinetti et al., Rev. of Scien. Instr. **83** (2012) 013506
[11] D. Kim et al., Plasma Phys. Control. Fusion **58** (2016) 055002
[12] M. Erba et al., Plasma Phys. Control. Fusion **39** (1997) 261
[13] L. Frassinetti et al., PPCF **59** (2017) 014014
[14] C. Angioni et al., Nucl. Fusion **47** (2007) 1326
[15] M.N.A Beurskens et al, Nucl. Fusion **54** (2014) 043001
[16] L. Frassinetti et al., Nucl. Fusion **57** (2017) 016012
[17] T. Tala et al., Proc. of the 26th IAEA Fusion Energy Conference (FEC 2016), Kyoto, EX/P6-12
[18] O. Sauter et al., Phys . Plasmas **6** (1999) 2834
[19] R. Hager et al., Phys Plasmas **23** (2016) 042503
[20] M. Romanelli et al. Plasma and Fusion Research **9** (2014) 3403023
[21] O. Meneghini et al., Phys. Plasmas **23** (2016) 042507
[22] C.F. Maggi et al., Nucl. Fusion **55** (2015) 113031
[23] C.D. Challis et al., Nucl. Fusion **55** (2015) 053031
[24] R.J. Goldston et al., J. Comput. Phys. **43** (1981) 61
[25] ITER Physics Basis Editors et al Nucl. Fusion **39** (1999) 2137
[26] H-S Bosch & G M Hale Nucl Fusion **32** (1992) 661
[27] D R Mikkelsen Nucl Fusion **29** (1989) 1113
[28] C.F. Maggi et al. Proc. 44rd EPS Conference on Plasma Physics, 26 - 30 June, 2017, Belfast, UK, to be submitted to Plasma Phys. Contr. Fusion.